GRAPHENE OXIDE REINFORCED POLY(VINYL ALCOHOL) NANOCOMPOSITES

S. MORIMUNE[1], T. NISHINO[1]* and T. GOTO[2]
[1]Department of Chemical Science and Engineering, Graduate School of Engineering, Kobe University, Rokko, Nada, Kobe, Japan
[2]Mitsubishi Gas Chem. Inc., Niijyuku, Katsushika, Tokyo, Japan
*Takashi NISHINO (tnishino@kobe-u.ac.jp)

Keywords: *Graphene oxide, Poly(vinyl alcohol), Nanocomposites, Young's modulus, Strength*

1 Introduction

The first major success of polymer nanocomposites, where the filler has at least one dimension in the nanoscale, was reported by Kojima, Usuki *et al.* [1] from the Toyota Central R&D group. They demonstrated that nylon6/clay nanocomposites showed significant improvement in the mechanical and the thermal properties. Since then, works on the polymer nanocomposites have been conducted on a wide variety of polymer matrices, such as thermoplastics (styrenics, polyolefins), thermosetting polymers (epoxy resins and phenolics), as well as with various nanofillers, such as layered silicates and carbon-based nanomaterials. It was revealed that, using only a small amount of nanofillers, these nanocomposites show remarkable enhancement in materials properties, including mechanical properties [2,3], thermal properties [4] and gas-barrier properties [5], compared with the virgin polymers or conventional microfillers composites.

In the last few decades, a variety of carbon-based nanomaterials, such as carbon nanotubes (CNTs) and fullerene have gained considerable attentions as nanofillers for the polymer nanocomposites because of their outstanding properties. For example, CNTs have been considered to be an ideal candidate for the reinforcement of polymer composites to enhance the mechanical, electrical, and thermal properties [6]. However, the success in imparting their amazing properties to the composites has been limited because of their tendency to form bundled agglomerates in the polymer matrices. In addition, their high cost, allegation against biosafety and the blackening of the products have been hampering their applications.

Recently, nanodiamond (ND) has been produced and it has been exploited in some fields of nanotechnology as a new carbon-based nanomaterial [7-9]. We reported that ND achieved the high dispersibility in poly(vinyl alcohol) (PVA) matrix by using a simple casting method from aqueous medium. The resulting nanocomposites had excellent properties derived from ND, which can approach the values of single-crystal diamond [10].

Graphene, a two dimensional sheet of covalently bonded sp^2 carbon atoms, has attracted a great deal of attention since the single sheet of graphene was isolated by Geim et. al. [11] The enormous amount of research has been made and the unique structure and properties of graphene were revealed [12]. One of the functionalized graphene materials, graphene oxide (GO), bears oxygen-containing functional groups on basal planes and edges of graphene. These groups attach the desired characteristic of water dispersibility to the pristine graphene sheet. Therefore, GO can be expected to be well-dispersed in polymer matrices and improve the issues of the conventional polymer/carbon-based materials.

In this study, GO-reinforced PVA nanocomposites were prepared by a simple casting method from aqueous medium. The structure and properties of the PVA/GO nanocomposites were investigated.

2 Sample preparation

Materials. Poly(vinyl alcohol) (PVA) was kindly supplied from Nippon Synthetic Chemical Industry Co., Ltd. with its commercial name "Gohsenol NH-18". The degree of polymerization was 1800 and the degree of saponification was more than 99 %. GO aqueous suspension (GO content = 1 wt%) was supplied from Mitsubishi Gas Chem. Inc.

Synthesis of PVA/GO nanocomposites. PVA powder was dissolved in distilled water at 90 ºC for 3 h. GO aqueous suspension was added to the PVA solution under vigorous stirring. The GO content was controlled by changing the amount of PVA (0, 0.1, 0.5, 1 and 5 wt%) added. The PVA/GO aqueous suspension was cast into a petri dish and dried at room temperature, then in vacuum at 40 ºC for 48 h. The film thickness was controlled as 100 μm.

3 Results and discussion

Fig. 1 shows the X-ray diffraction profiles of the PVA film, the PVA/GO nanocomposites and GO. The characteristic diffraction peak of GO appeared clearly at 2θ = 11.1 º which can be assigned as 001 reflection arose from graphite interlayer. This suggests that GO formed agglomerates during drying process from the aqueous suspension. On the other hand, for the nanocomposites, this reflection disappeared. It was revealed that GO was well exfoliated and homogeneously dispersed in the PVA matrix [13]. The crystallinity (X_c) of PVA for the PVA/GO nanocomposites increased by the incorporation of GO from 28 % of the neat PVA film to 30, 33, 35 and 39 % by 0.1, 0.5, 1 and 5 wt% GO loading, respectively. GO was considered to act as the crystallization nucleus for PVA, thus, the micro structure of PVA matrix was affected by adding GO.

Fig. 2 shows the stress (σ)-strain (ε) curves of the PVA film and the PVA/GO nanocomposites. The tensile strength (σ_{max}), equal to the yielding stress, and the Young's modulus (E) dramatically increased by the incorporation of GO. While the PVA film showed the typical σ-ε curve for the conventional polymer film with yielding, the elongation at break (ε_{max}) of the nanocomposites decreased with the increasing of the GO content,. However, for the nanocomposites with 0.1 wt % GO loading, the high ε_{max} close to that of the PVA film remained. Therefore, toughness (K) of the nanocomposites with 0.1 wt% GO loading increased 33 % higher than that of the PVA film. Zhao *et al.* [14] reported that the slippage of graphene nanosheets during the tensile testing will suppress the rapid decreasing of the ε_{max}. It can be assumed that as further adding GO into the PVA matrix, the interaction between GO sheets, mainly by van der Waals force, stack the sheets together and GO form agglomerates. Therefore the brittle failure easily occurred at the interface between PVA matrix and GO.

Fig. 3 shows the relationship between the E value and the GO content of the PVA/GO nanocomposites. The E value of the nanocomposite increased drastically, for example, 76 % increase compared with those of PVA film was observed for the composite with only 0.1 wt% GO loading. We compared experimental data with the model predictions for the PVA/GO nanocomposites using Halpin-Tsai equations, the most widely used model to estimate reinforcement effect of filler in composites, based on the assumption that GO sheets aligned parallel to the surface of the composite films [15]. The equations are given as follows:

$$E_c = E_m \frac{(1+\eta\xi V_f)}{(1-\eta V_f)} \quad (1)$$

$$\eta = \frac{(E_m/E_c - 1)}{(E_m/E_c + \xi)} \quad (2)$$

E_c, E_f, E_m : E of the composites, filler and matrix, respectively.

V_f : Volume fraction of filler.

ξ is a shape parameter depends on filler geometry, orientation and loading direction and equals to the following equation:

$$\xi = \frac{2\alpha_f}{3} = \frac{2l_f}{3t_f} \quad (3)$$

l_f : Length of GO, t_f : Thickness of GO.

The calculated result is also shown in Fig. 3 with the dotted line. For the nanocomposites with the low content of GO, under 0.5 wt%, the experimental E value greatly exceeded the model predictions. These unrivaled reinforcement effects can be achieved by the combination of several extra elements in the PVA/GO nanocomposites. First of all, as previously mentioned in Fig. 1, the X_c of PVA matrix increased with the increasing of GO content. Therefore the mechanical properties of PVA matrix in the nanocomposites increased, which contributed to the increase of overall mechanical properties. In addition, the large aspect ratio of the GO sheet, together with that of nanodispersion in the matrix, contributes to the strong interfacial interaction, mainly by hydrogen bonding, between GO sheet and PVA [16]. On the other hand, for the nanocomposites with GO content of 5 wt%, the experimental E value was below the calculated one. The fracture of the

nanocomposites was considered to be caused by the aggregation of GO in the PVA matrix.

Fig. 4 shows the thermogravimetric traces of the PVA film and the PVA/GO nanocomposites under N_2 flow. The onset temperature of the thermal degradation of the nanocomposite with 1 wt% GO loading was about 10 ºC higher than that of the PVA film. This indicates that the nanodispersion of GO can act as a barrier to volatile the decomposition products throughout the composites with its plate-like configuration, thus the thermal stability can be improved by the incorporation of GO.

Since the polymer/clay nanocomposite was exploited, due to the high aspect ratio of clay, the improvements in barrier properties have been revealed. As well as clay, GO sheet possesses high aspect ratio and the effective barrier properties can be expected.

Fig. 5 shows the swelling ratio of the PVA film and the PVA/GO nanocomposites in distilled water at 30 ºC. The swelling ratio was suppressed drastically by the incorporation of GO. For the nanocomposite with 1 wt% loading of GO, the swelling ratio decreased by 70 %. This indicates that the penetration pass of water in the PVA matrix was prolonged by the nanodispersion of the GO sheet together with their high aspect ratio. Furthermore, GO sheet suppressed molecular motion of PVA sufficiently. Therefore, not only the properties of GO, the unique structure, the sheet-like structure, of GO was effectively imparted to the nanocomposites.

4 Conclusions

We prepared PVA/GO nanocomposites by a simple casting method from aqueous medium. From the XRD analysis, GO was found to be exfoliated and nano-dispersed and the crystallinity of PVA was increased. For the mechanical properties, the Young's modulus and the tensile strength dramatically increased compared with those of PVA film. Especially at a low content of GO, the experimental *E* value increased much above the model prediction. It was revealed that GO bound strongly with PVA mainly by hydrogen bonding. In addition, the thermal properties and barrier property remarkably increased when the GO particles were incorporated. These were largely attributed to the rigid and sheet-like configuration of GO. In conclusion, we succeeded to impart the excellent properties of GO to the PVA matrix and create the remarkable nanocomposites.

References

[1] Y. Kojima, A. Usuki, M. Kawasumi, A. Okada, Y. Fukushima, T. Karauchi, O. Kamigaito, "Synthesis of nylon 6-clay hybrid", *J. Mater. Res.*, Vol. 8, No. 5, pp 1179-1184, 1993.

[2] Y. Kojima, A. Usuki, M. Kawasumi, A. Okada, Y. Fukushima, T. Karauchi, O. Kamigaito, "One-pot synthesis of nylon 6–clay hybrid", *J. Polym. Sci. Part A: Polym Chem*, Vol. 31, No. 7, pp 1755-1758, 1993.

[3] S. Morimune, M. Kotera, T. Nishino, " Stress transfer of poly (vinyl alcohol) / montmorillonite nanocomposite using X-ray diffraction**,** *Journal of the Adhesion Society of Japan*, Vol. 46, No. 9, pp 320-325, 2010.

[4] C. Wei, D. Srivastava, K. Cho, "Thermal Expansion and Diffusion Coefficients of Carbon Nanotube-Polymer Composites", *Nano Lett*., Vol. 2, No. 6, pp 647-650, 2002.

[5] T. Lan, P. D. Kaviratna, T. J. Pinnavaia, "On the Nature of Polyimide-Clay Hybrid Composites", *Chem. Mater.*, Vol. 6, No. 5, pp 573-575, 1994.

[6] B. E. Kilbride, J. N. Coleman, P. Fournet, M. Cadek, A. Drury, W. J. Blau, "Experimental observation of scaling laws for alternating current and direct current conductivity in polymer-carbon nanotube composite thin films", *J. Appl. Phys.* , Vol. 92, No. 7, pp 4024-4030, 2002.

[7] R. Greiner, D. S. Phillips, J. D. Johnson, A. F. Volk, "Diamonds in detonation soot", *Nature*, Vol. 333, pp No. 6172, 440-442, 1988.

[8] R. Lam, M. Chen, E. Pierstorff, H. Huang, E. Osawa, D. Ho, "Nanodiamond Embedded Microfilm Devices for Localized Chemotherapeutic Elution", *ACS Nano*, Vol. 2, No. 10, pp 2095-2102, 2008.

[9] K. D. Behler, A. Stravato, V. Mochalin, G. Korneva, G. Yushin, Y. Gogotsi, "Nanodiamond-polymer composite fibers and coatings.", *ACS Nano*, Vol. 3, No. 2, pp 363-369, 2009.

[10] S. Morimune, M. Kotera, T. Nishino, K. Hata, K. Goto, "Poly(vinyl alcohol) Nanocomposites with Nanodiamond", *Macromolecules*, DOI: 10.1021/ma200176r, 2011.

[11] K. S. Novoselov, A. K. Geim, S. V. Morozov, D. Jiang, Y. Zhang, S. V. Dubonos, I. V. Grigorieva, A. A. Firsov, "Electric Field Effect in Atomically Thin Carbon Films", *Science*, Vol. 306, No. 5696, pp 666-669, 2004.

[12] H. Kim, A. Abdala, C. Macosko, "Graphene/Polymer Nanocomposites", *Macromolecules*, Vol. 43, No. 16, pp 6515-6530, 2010.

[13] J. Liang, Y. Houng, L. Zhang, Y. Wang, Y. Ma, T. Guo, Y. Chen, "Molecular-Level Dispersion of Graphene into Poly(vinyl alcohol) and Effective Reinforcement of their Nanocomposites", *Adv. Funct. Mater*, Vol. 19, No. 14, pp 2297-2302, 2009.

[14] X. Zhao, Q. Zhang, D. Chen, P. Lu, "Enhanced Mechanical Properties of Graphene-Based Poly(vinyl alcohol) Composites", *Macromolecules*, Vol. 43, No. 5, pp 2357-2363, 2010.

[15] J. C. Halpin, J. L. Kardos, "The Halpin-Tsai Equations: A Review", *Polym. Eng. Sci.*, Vol. 16, No. 5, pp 344-352, 1976.

[16] Y. Xu, W, Hong, H. Bai, C. Li, G. Shi, "Strong and ductile poly(vinyl alcohol) graphene oxide composite films with a layered structure", *Carbon*, Vol. 47, No. 15, pp 3538-3543, 2009.

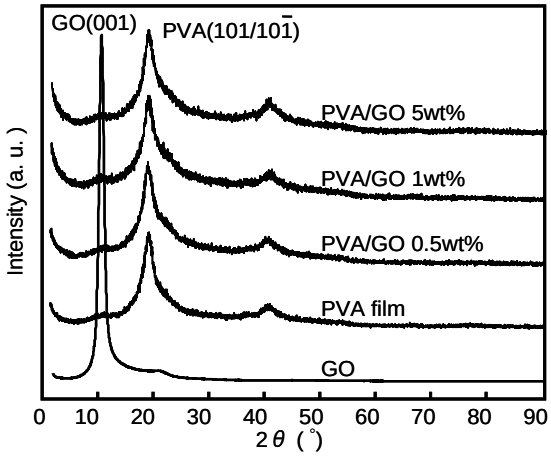

Fig. 1 X-ray diffraction profiles of PVA/GO nanocomposites.

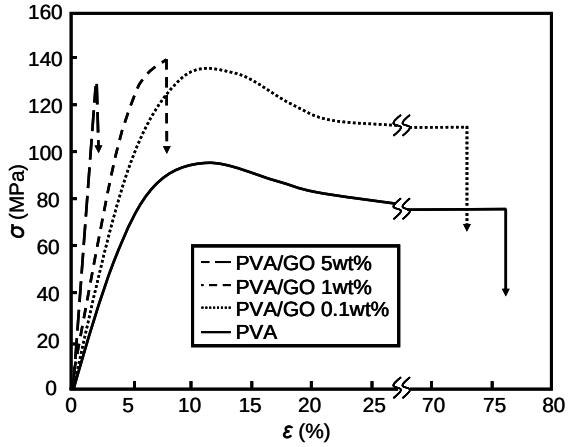

Fig. 2 Stress (σ)-strain (ε) curves of PVA/GO nanocomposites.

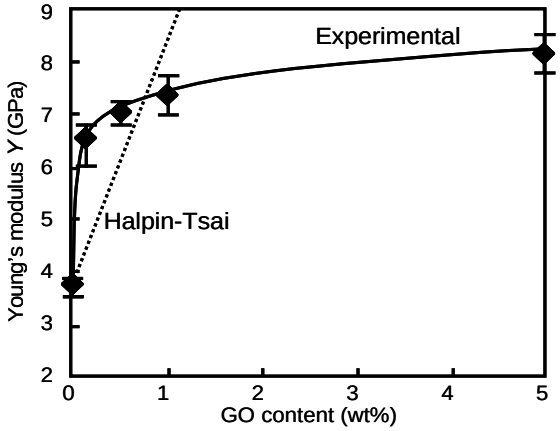

Fig. 3 Experimental Young's modulus (E) of PVA/GO nanocomposites and calculated data derived from the Halpin-Tsai equation.

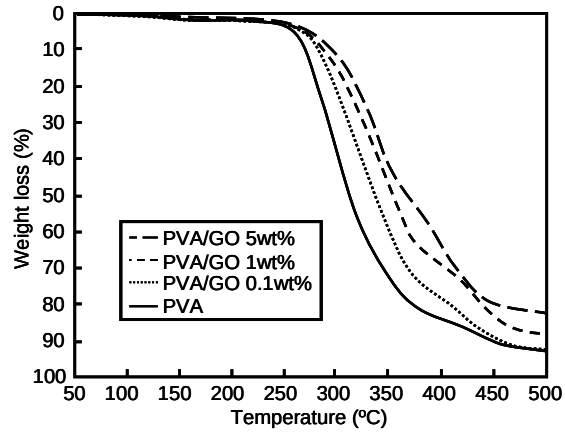

Fig. 4 Thermogravimetric traces of PVA/GO nanocomposites.

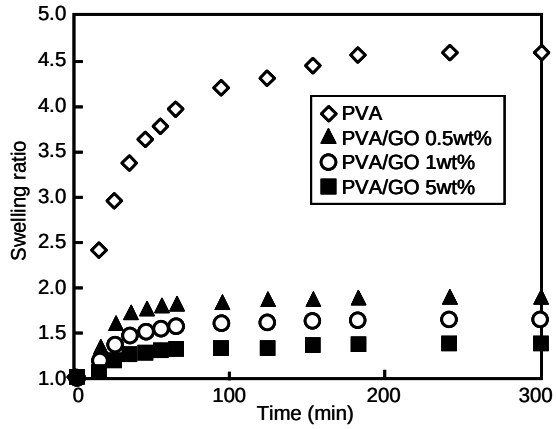

Fig. 5 Swelling ratio of PVA/GO nanocomposites in distilled water at 30 ºC.